

# Stable, Glassy, and Versatile Binaphthalene Derivatives Capable of Efficient Hole Transport, Hosting, and Deep-Blue Light Emission

By Bin Wei, Ji-Zhong Liu, Yong Zhang, Jian-Hua Zhang, Hua-Nan Peng, He-Liang Fan, Yan-Bo He, and Xi-Cun Gao\*

Organic light-emitting diodes (OLEDs) have great potential applications in display and solid-state lighting. Stability, cost, and blue emission are key issues governing the future of OLEDs. The synthesis and photoelectronics of a series of three kinds of binaphthyl (BN) derivatives are reported. BN<sub>1-3</sub> are “melting-point-less” and highly stable materials, forming very good, amorphous, glass-like films. They decompose at temperatures as high as 485–545 °C. At a constant current density of 25 mA cm<sup>-2</sup>, an ITO/BN<sub>3</sub>/Al single-layer device has a much-longer lifetime (>80 h) than that of an ITO/NPB/Al single-layer device (8 h). Also, the lifetime of a multilayer device based on BN<sub>1</sub> is longer than a similar device based on NPB. BNs are efficient and versatile OLED materials: they can be used as a hole-transport layer (HTL), a host, and a deep-blue-light-emitting material. This versatility may cut the cost of large-scale material manufacture. More importantly, the deep-blue electroluminescence (emission peak at 444 nm with CIE coordinates (0.16, 0.11), 3.23 cd A<sup>-1</sup> at 0.21 mA cm<sup>-2</sup>, and 25200 cd m<sup>-2</sup> at 9 V) remains very stable at very high current densities up to 1000 mA cm<sup>-2</sup>.

## 1. Introduction

Organic light-emitting diodes (OLEDs) have been extensively studied due to their great potential in flat-panel displays and as a solid-state lighting source.<sup>[1]</sup> However, some of the critical factors, such as stability, cost and blue-emitting materials/devices, have

not yet been fully resolved and still govern large-scale OLEDs' marketing.

As to the first issue, there are many intrinsic and extrinsic factors that affect the lifetime of OLEDs, such as electrochemical and interfacial degradation, coverage of particles, and encapsulation. Detailed investigations have been undertaken and efforts from a physical point of view such as doping of the hole-transport layer (HTL),<sup>[2]</sup> introducing a CuPc buffer layer at the hole-injecting contact,<sup>[3]</sup> or using a mixed emitting layer,<sup>[4]</sup> modifying the indium tin oxide (ITO) surface,<sup>[5]</sup> encapsulation,<sup>[6]</sup> and driving strategies<sup>[7]</sup> have been made to improve OLED stability. Although recent studies have confirmed the instability of the cationic tris(8-hydroxyquinolato)aluminum (Alq<sub>3</sub>) species at the *N,N'*-bis-(1-naphthyl)-*N,N'*-diphenyl-1,1'-biphenyl-4,4'-diamine (NPB)/Alq<sub>3</sub> interface as one of the main device-degradation mechanisms for

small-molecule Alq<sub>3</sub>-based OLEDs,<sup>[8]</sup> many reports have revealed that the morphological instability of the hole-transport layer is responsible for the device lifetime, especially at higher temperatures, and, from the synthetic organic chemistry point of view, many hole-transporting materials with high glass-transition temperatures (*T<sub>g</sub>*) have been synthesized.<sup>[9]</sup> This is very important because such devices not only need to be operated at high temperatures sometimes but also need to be operated at high current densities with high luminance in the lighting source. In these circumstances, materials with a high *T<sub>g</sub>* are better, to be able to resist heat. In addition, not all OLED devices are Alq<sub>3</sub>-based. Blue-, red- or white-light-emitting devices do not necessarily use the NPB/Alq<sub>3</sub> interface. Therefore, materials with a high glass-transition temperature are still highly desirable.

As to the second issue, the cost of manufacturing OLEDs mainly comes from the synthesis of the materials and the fabrication of the devices. On the materials-synthesis side, up to now, OLED materials with various colors, including blue, green, red, and white light, and various functions including hole injection and transport, electron injection and transport guest and host, fluorescence and phosphorescence, have been synthesized. For full-color displays and white-lighting, many kinds of materials with great quantities are needed. One way to reduce the cost of materials synthesis is large-scale-

[\*] Prof. X. C. Gao  
Department of Chemistry, School of Science, Nanchang University  
999 Xue-Fu Road, Hong-Gu-Tan New District, Nanchang 330031  
(China)  
and  
State Key Lab of Silicon Materials, Zhejiang University  
Hangzhou 310027 (China)  
E-mail: xcgao@ncu.edu.cn

Prof. B. Wei, J. Z. Liu, Y. Zhang, Prof. J. H. Zhang  
Key Laboratory of Advanced Display and System Applications  
Ministry of Education, Shanghai University  
P. O. B. 143, 149 Yanchang Road, Shanghai 200072 (China)

Prof. X. C. Gao, H. N. Peng, H. L. Fan, Y.-B. He  
Department of Chemistry, School of Science, Nanchang University  
999 Xue-Fu Road, Hong-Gu-Tan New District, Nanchang 330031  
(China)

DOI: 10.1002/adfm.201000299



yield of BN<sub>1-3</sub> of the total three steps was 30%, 35% and 22% respectively.

## 2.2. Measurements

The <sup>1</sup>H NMR spectra were collected using a Bruker 400 MHz spectrometer. The absorption spectra were obtained using a Perkin–Elmer Lambda-35 UV-vis spectrometer. The photoluminescence (PL) spectra were collected using a Hitachi F-4500 fluorescence spectrophotometer. The PL emission quantum yields (PLQYs) were measured at room temperature in dichloromethane solution. Quinine in 1.0 N H<sub>2</sub>SO<sub>4</sub> ( $\Phi = 0.48$  at 313 nm) was used as a reference.<sup>[14]</sup> To obtain the quantum-yield data as precisely as possible, the absorption and PL had to be measured in a single machine run to compare the integrated emission areas. The difference between the refractive index of the solvent and that of the standard should also be counted. Differential thermal analysis (DTA) and thermogravimetric analysis (TGA) were performed on a Perkin–Elmer MAS-5800 instrument with a heating/cooling rate of 10 °C min<sup>-1</sup> and a nitrogen flow rate of 90 ml min<sup>-1</sup>. Cyclic voltammetry (CV) was performed on a CHI 600C instrument in anhydrous *N,N*-dimethylformamide (DMF) containing 0.1 M (Bu)<sub>4</sub>NClO<sub>4</sub> as the supporting electrolyte at a scan rate of 100 mV s<sup>-1</sup>. The working electrode was glass carbon and the reference electrode was Ag/AgCl. Atomic force microscopy (AFM) measurements were performed in the tapping mode under ambient conditions using a SPI 4000 instrument.

## 2.3. Device Fabrication

The devices were fabricated by conventional vacuum deposition of the organic layers and cathode onto an ITO-coated glass substrate under a base pressure lower than  $5 \times 10^{-6}$  Torr. Al was used as the cathode. The ITO was cleaned by UV-ozone treatment at 150 °C. The entire organic layers and the Al cathode were deposited without exposure to the atmosphere. The deposition rates for the organic materials, LiF, and Al were typically 0.1, 0.025, and 0.5 nm s<sup>-1</sup>, respectively.

## 2.4. Device Measurement

The devices were measured with a Hewlett–Packard 4140B source measure unit and a PR-650 luminance color meter. The color meter was placed on the bottom of the test device to measure the front luminance. The fluorescence spectra were recorded using a Jasco FP-75 spectrophotometer. For the lifetime measurements, the devices were encapsulated with glass lids under a N<sub>2</sub> atmosphere. The voltage rise and luminance degradation were recorded simultaneously every hour.

## 2.5. Glassy Materials for Amorphous Films and Stable Devices

The stability of OLED devices is governed by many factors. Although some of them are not yet fully known, advanced amorphous materials especially the hole-transporting materials mainly developed by Shirota's group are often designed to increase

the thermal stability of the material and overall efficiency of the device, to resist Joule heating.<sup>[15]</sup> In general, the wise choice and design of advanced materials with high thermal stability, very good carrier-transport ability and matched energy levels are undoubtedly the basis for a well-performed, stable device. Figure 1 compares the thermal properties of BN<sub>1-3</sub> with those of NPB, measured by DTA and TGA. The TGA results indicate that BN<sub>1-3</sub> exhibit *T*<sub>d</sub> of 485, 492, and 545 °C, respectively, while *T*<sub>d</sub> for NPB is only 410 °C. This high thermal stability apparently derives from the molecular structure of the bulky binaphthyl backbone that retards the stretching and rotating of the molecules and sucks the thermal energy. In addition, the DTA curves for BN<sub>1-3</sub> show no apparent endothermal incidents in the whole heating process from room temperature up to the decomposition of the materials, while for NPB, there is an evident endothermal peak at 280 °C corresponding to its melting point. We did not observe any apparent sharp melting phenomena for the BNs under the microscope of the lab-use melting-point-measurement instrument. This means the BNs have neither a melting point nor a glass-transition temperature. This is a very peculiar character for small-molecule materials. As we know, though the glass-transition temperature cannot be easily determined for all materials, the melting point for almost all small organic materials is definite. These “melting-point-less” materials may imply highly amorphous films. The melting point of a solid is the temperature range at which its state changes from solid to liquid. A solid can be regarded as a highly organized, frozen, or crystallized liquid; a liquid can be regarded as a highly disordered, melted, or amorphous solid. Some materials, such as glass, may harden without crystallizing and they are called amorphous solids. Amorphous materials, including some polymers, do not have a true melting point as there is no abrupt phase change at any specific temperature. Instead, there is a gradual change in their viscoelastic properties over a range of temperatures. Such materials are characterized by a glass-transition temperature referring to the transformation of a glass-forming liquid into a glass, which usually occurs upon rapid cooling. Structurally, the bulky binaphthyl unit makes the whole molecule possess a non-coplanar configuration that results in a decreased tendency to crystallize and weaker intermolecular interactions in the solid state, leading to their pronounced morphological stability and high quantum efficiency (Section 2.8). These materials can now, in a sense, be said to be polymeric small molecules. Figure 2 shows photos taken using an ordinary digital camera and a fluorescence microscope. They look like real transparent and fluorescent glasses.

AFM further proves the thermal stability and amorphism. Figure 3 compares the topography of the NPB film and the BN<sub>1-3</sub> films under different temperatures. The NPB film crystallized at 100 °C in 20 minutes. For BN<sub>1</sub>, the roughness changed from 0.257 nm at room temperature to 0.550 nm at 100 °C. Although at higher temperature, 150 °C, the roughness changed to 1.239 nm, the morphology seemed much flatter than that of NPB. For BN<sub>3</sub>, the fluorine-substituted carbazole groups made the film keep much-better amorphism even than BN<sub>1</sub> at a very high annealing temperature, 300 °C, with the roughness changing from 0.228 nm to only 0.272 nm. For BN<sub>2</sub>, the morphology seemed flattened with a significant change, however: it was rather glass like, than crystallized, like NPB.

To test the device stability, we omitted the Alq<sub>3</sub> layer and fabricated single-layered devices (unpacked), because we were

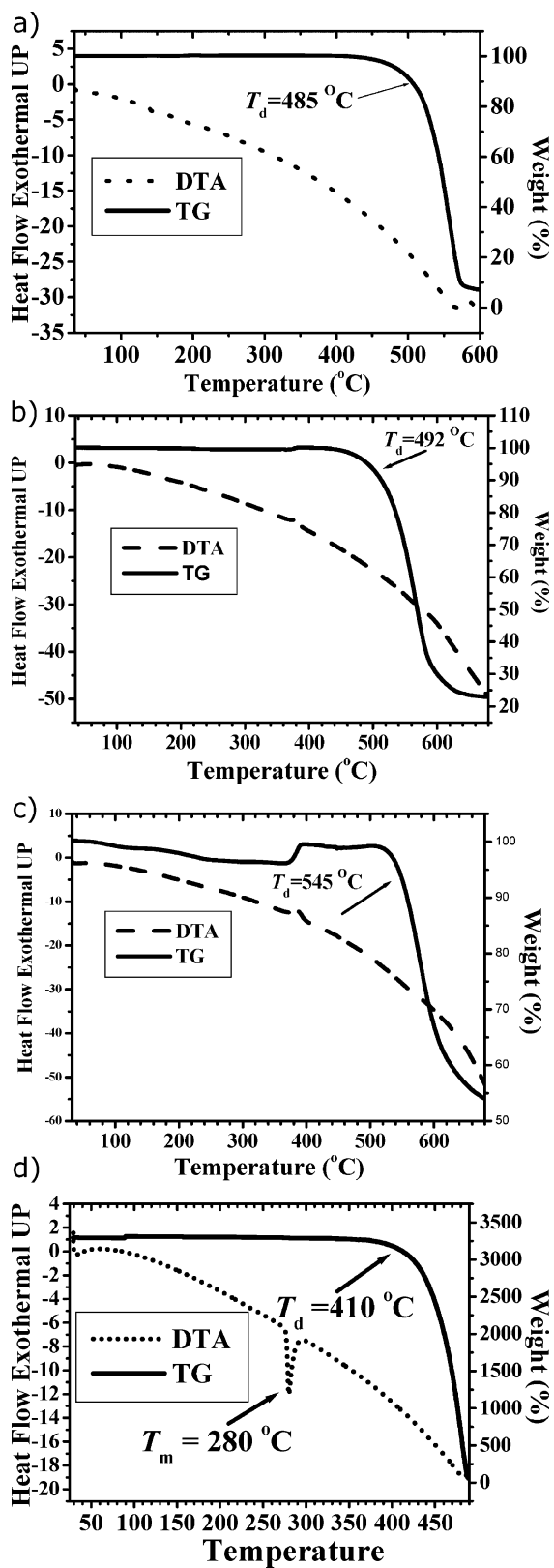


**Figure 1.** a) DTA and TGA curves for BN<sub>1</sub>. b) DTA and TGA curves for BN<sub>2</sub>. c) DTA and TGA curves for BN<sub>3</sub>. d) DTA and TGA curves for NPB. The sudden change at  $\sim 380\text{ }^\circ\text{C}$  for BN<sub>3</sub> derives from instrumental noise.

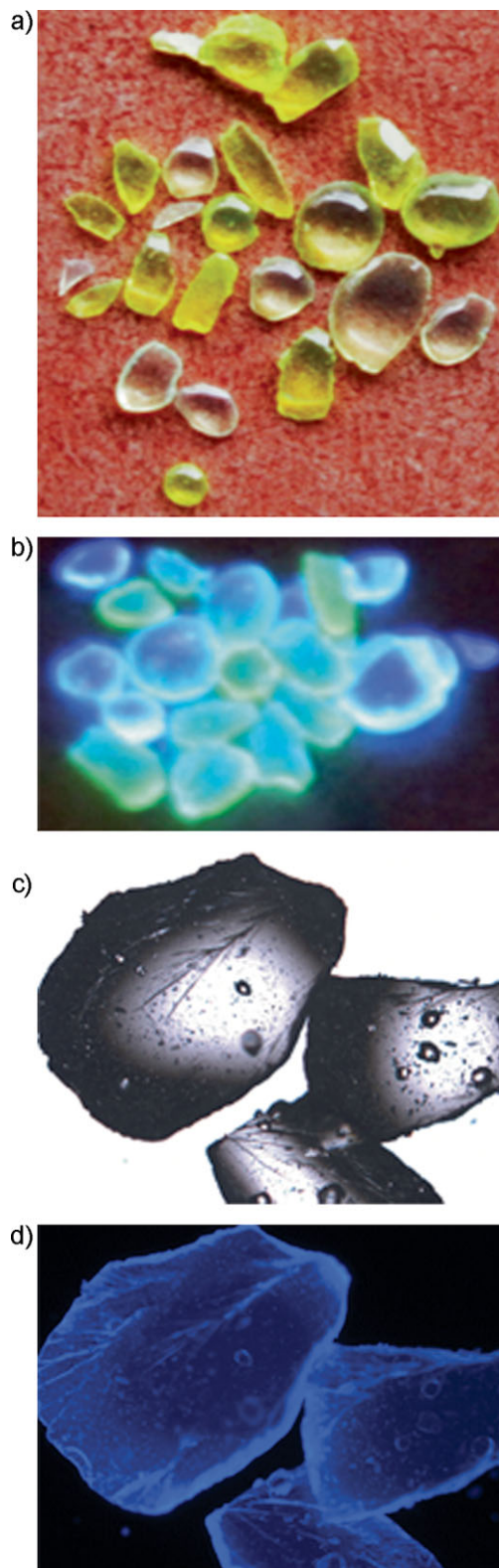


**Figure 2.** a) Photo of the vacuum-sublimed BN<sub>1</sub> sample. b) Photo of the vacuum-sublimed BN<sub>1</sub> sample under 365 nm UV excitation. c) Photo of the vacuum-sublimed BN<sub>2</sub> sample taken using a Leica DM 5000B microscope 5 $\times$ . d) Photo of the vacuum-sublimed BN<sub>2</sub> sample taken using a Leica DM 5000B microscope 5 $\times$  under UV excitation.

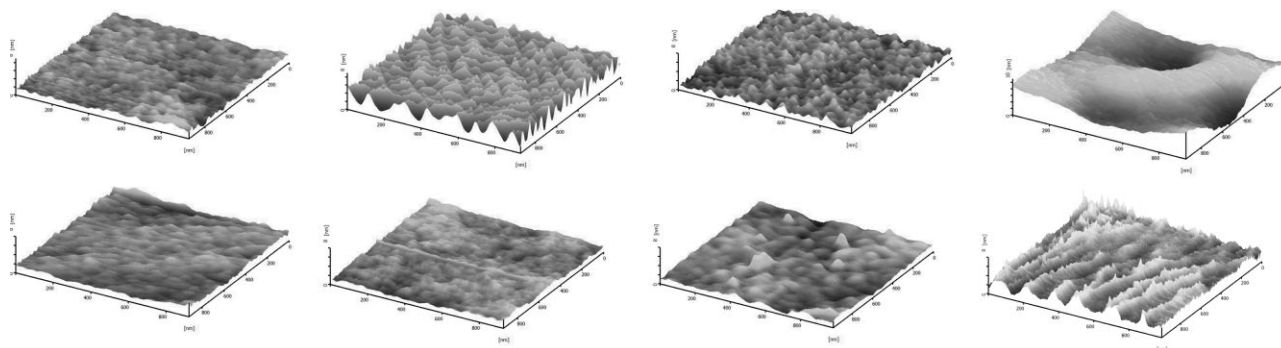


**Figure 3.** Comparison of the AFM images of the NPB, and the BN<sub>1–3</sub> thin films (60 nm) at room temperature and under different annealing temperatures (20 minutes). The top row from left to right: NPB, BN<sub>1</sub>, BN<sub>2</sub>, BN<sub>3</sub> at room temperature; the bottom row from left to right: NPB 100 °C, BN<sub>1</sub> 150 °C, BN<sub>2</sub> 150 °C, BN<sub>3</sub> 300 °C.

worried that Alq<sub>3</sub> might disturb the film. From Figure 4, we see that the voltage for the NPB-based device increased very early (at ambient temperature). In a period of only 8 h, the device became short-circuited due to some kind of crystallization, while the voltage for the BN<sub>1</sub>-based device kept constant for a much-longer time (more than 80 h). Therefore, the BN<sub>1</sub>-based single-layer device was much-more stable than the NPB-based single-layer device.

## 2.6. As a HTL Material and the Device Stability

The OLED device structure is usually multilayered, where each component is equally important. For HTL materials, amorphous amines are the most widely and successfully used.<sup>[15]</sup> Our amines, as HTLs, were first determined by the CV curves of their highest-occupied-molecular-orbital (HOMO) levels, with those for NPB and BN<sub>1–3</sub> being 5.47, 5.67, 5.97, and 5.71 eV respectively. Especially for BN<sub>1</sub>, the CV curve was completely reversible. This reversibility means very good electrochemical stability and can contribute to the device stability in the end.<sup>[16]</sup> Apparently, these binaphthalene derivatives possess higher HOMO levels than NPB, which may result in difficulties for holes to be injected from the

ITO. However, that is not the end of the story. The emission efficiency of an OLED is dependent not only on the hole injection, but also on the hole-electron pair recombination. Besides, we can insert a “ladder” layer (which can also be called a buffer or hole injection layer (HIL) layer) between the ITO and the HTL to assist hole injection to the HTL with the higher HOMO level. In single-layer cells, as illustrated in Figure 5, we can see that the current density plotted against electric field for the BN<sub>1</sub>-based hole-only device coincided very well with that of an Alq<sub>3</sub>-based electron-only device. The carrier mobility was electric-field dependent.<sup>[17]</sup> Under both low and high electric fields, the current density of the BN<sub>1</sub> matched very well with that of Alq<sub>3</sub>. Therefore, this well-matched carrier injection may counteract the effect of the higher HOMO level when BN<sub>1</sub> is used in the BN<sub>1</sub>/Alq<sub>3</sub>-based devices. This assumption was confirmed by the performance of the following real devices. In Figure 6, the BN<sub>2</sub>-based device is the poorest: it displays the lowest current density, luminance and efficiency. This clearly proves the difficulty for holes to be injected into BN<sub>2</sub>, which has the highest HOMO level of the three BNs. For the BN<sub>1,3</sub>-based devices at high voltage, the current density increased quickly and the luminance and efficiency surpassed those of the NPB-based device. Especially for the BN<sub>1</sub>-based device, the highest efficiency reached 8.03 cd A<sup>-1</sup>, more than 3 times higher than that of the

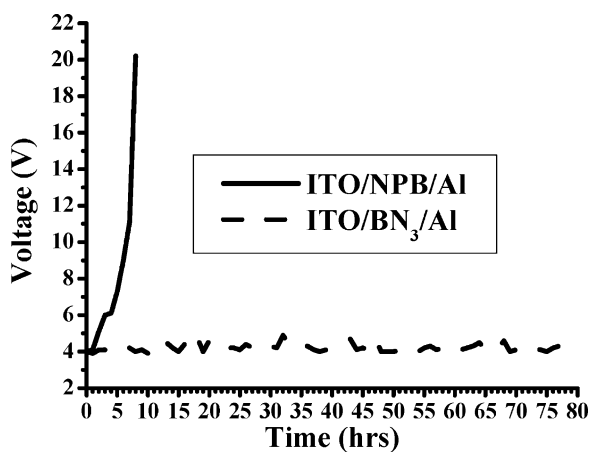


**Figure 4.** Stability test: voltage output of the devices in air under a constant current density of 25 mA cm<sup>-2</sup>.

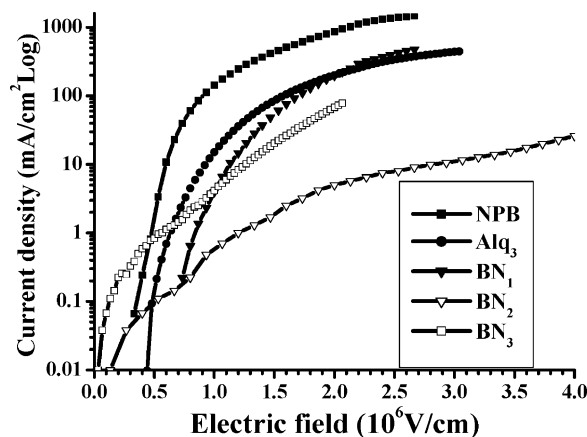


**Figure 5.** Current density vs. electric field for the hole-only devices, ITO/NPB or BN<sub>1–3</sub> (60 nm)/Au (50 nm), and the electron-only device, ITO/Alq<sub>3</sub> (60 nm)/LiF/AI (150 nm).

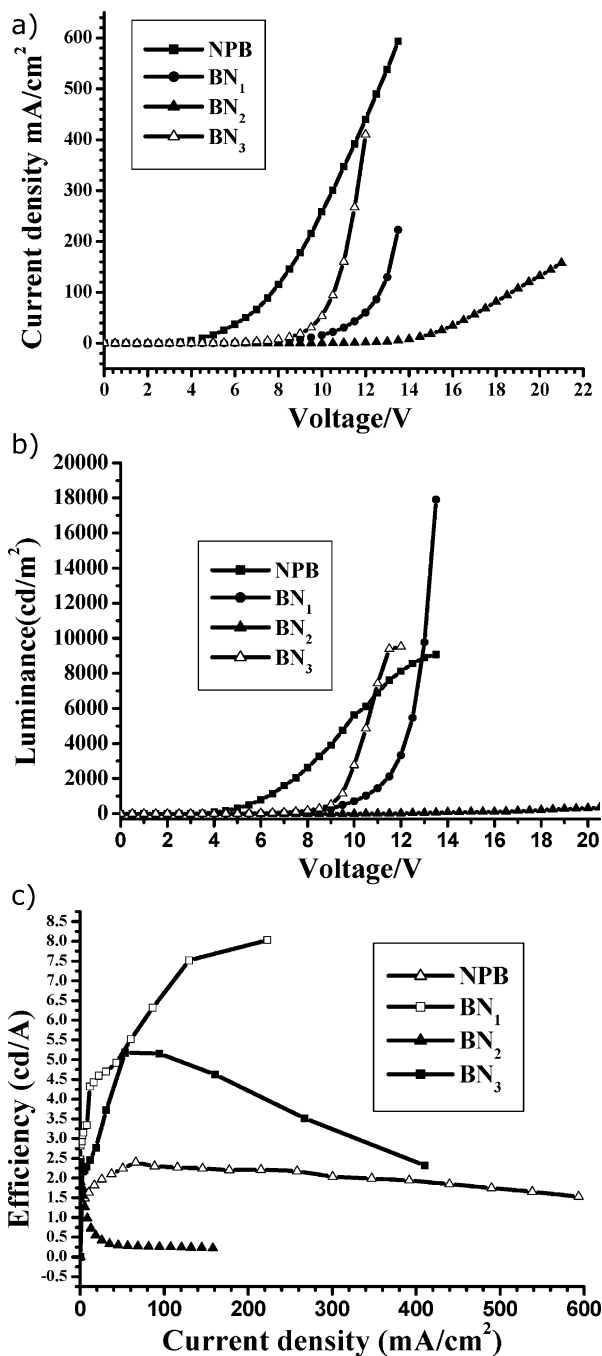


**Figure 6.** a) Current-density–voltage curves for the ITO/NPB or BN<sub>1–3</sub> (60 nm)/Alq<sub>3</sub> (60 nm)/LiF/Al (50 nm) devices. b) Luminance–voltage curves for the ITO/NPB or BN<sub>1–3</sub> (60 nm)/Alq<sub>3</sub> (60 nm)/LiF/Al (50 nm) devices. c) Efficiency–current-density curves for the ITO/NPB or BN<sub>1–3</sub> (60 nm)/Alq<sub>3</sub> (60 nm)/LiF/Al (50 nm) devices. In all of the devices, BN<sub>1–3</sub> functions as a HTL.

device with NPB as the HTL (2.39 cd A<sup>-1</sup>). In addition, the device performance with BN<sub>1</sub> and BN<sub>3</sub> as the HTL could be further improved by inserting a 30 nm NPB buffer layer. As shown in Figure 7, the current efficiency and maximum luminance of the ITO/NPB/BN<sub>1</sub>/Alq<sub>3</sub>/LiF/Al device were 9.48 cd A<sup>-1</sup> and 25 300 cd m<sup>-2</sup> respectively. Figure 8 compares the stability between

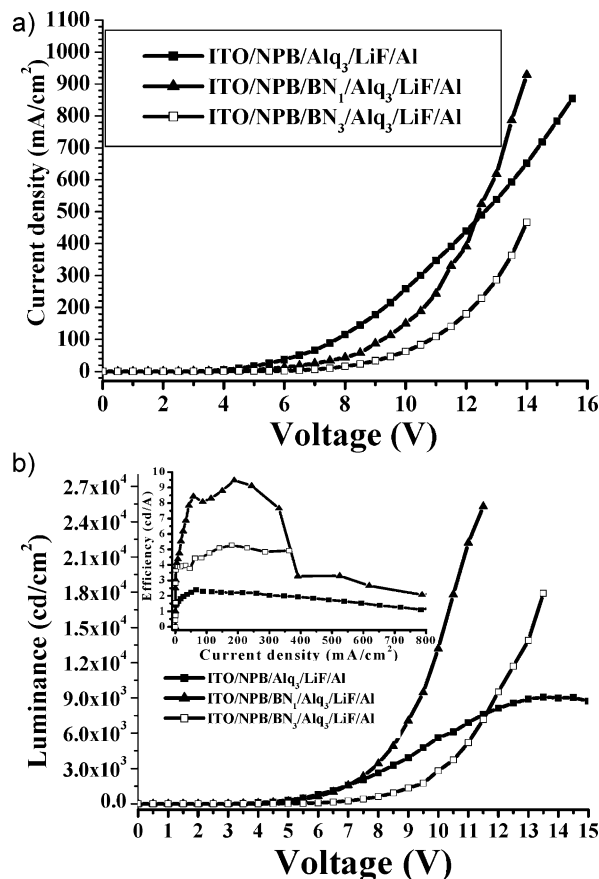


**Figure 7.** a) Current-density–voltage curve for the ITO/NPB (30 nm)/BN<sub>1,3</sub> (30 nm)/Alq<sub>3</sub> (60 nm)/LiF/Al (50 nm) devices. b) Luminance–voltage (and inset: efficiency–current-density) curves for the ITO/NPB (30 nm)/BN<sub>1,3</sub> (30 nm)/Alq<sub>3</sub> (60 nm)/LiF/Al (50 nm) devices. In all of the devices, BN<sub>1–3</sub> functions as the HTL and NPB as the HIL.

the sealed ITO/NPB/Alq<sub>3</sub>/LiF/Al and ITO/NPB/BN<sub>1</sub>/Alq<sub>3</sub>/LiF/Al devices. The half-lifetime (defined as the time elapsed before the luminance of the OLED decreases to half of its initial value) for the device with NPB as the sole HTL was 66 h and, for the device with NPB as the HIL and BN<sub>1</sub> as the HTL, was 110 h. The luminance decay for the latter device became much slower after the initial tens of hours. In addition, there was a sharp increase in the driving voltage for the former while for the latter, the driving-voltage increase was flatter. Therefore, we can say that an OLED device with BN<sub>1</sub> as the HTL material has a very-good lifetime.

## 2.7. As a Host Material

To avoid concentration quenching and enhance energy harvesting, fluorescent materials are often doped or solved in host materials, as guest materials. A principle for doing this is making a wise choice of the host material, which must be able to initiate effective energy harvesting and transfer to the guest. Practically, the emission from the host must have an efficient overlap with the absorption of the guest. However, this choice of host material is still awkward because there are indeed few host materials in stock: typically

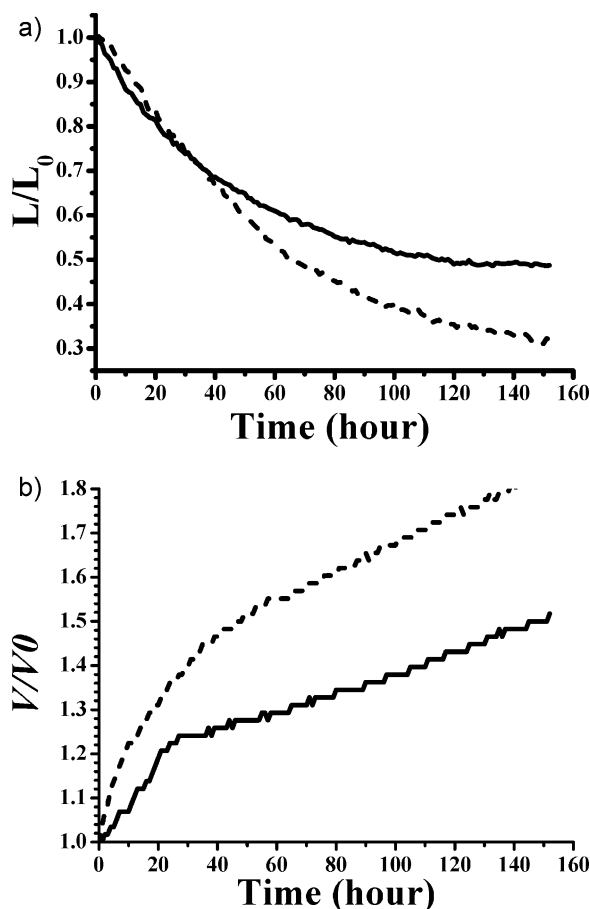


**Figure 8.** a) Luminance ( $L$ )/initial luminance ( $L_0$ ) for ITO/NPB (50 nm)/Alq<sub>3</sub> (60 nm)/LiF/Al (dashed line) and ITO/NPB (30 nm)/BN<sub>1</sub> (20 nm)/Alq<sub>3</sub> (60 nm)/LiF/Al (solid line). b) Driving voltage ( $V$ )/initial driving voltage ( $V_0$ ) vs. time for ITO/NPB (50 nm)/Alq<sub>3</sub> (60 nm)/LiF/Al (dashed line) and ITO/NPB (30 nm)/BN<sub>1</sub> (20 nm)/Alq<sub>3</sub> (60 nm)/LiF/Al (solid line). Both devices were driven at 20 mA cm<sup>-2</sup>. The  $L_0$  values were 485 cd m<sup>-2</sup> and 1176 cd m<sup>-2</sup>, respectively, for the former device and the latter.

4,4'-bis(*N*-dicarbazolyl)-1,1'-biphenyl (CBP), Alq<sub>3</sub>, 1,3,5-tris(*N*-phenylbenzimidazol-2-yl)benzene (TPBI), and 9,10-di(2-naphthyl)anthracene (AND).<sup>[18]</sup> Figure 9 compares the device performance of the coumarin 6 guest emitting material doped in CBP and BN<sub>1-3</sub> as host materials. Both the luminance and efficiency of the BN<sub>1-3</sub>-based devices were superior to those of the CBP-based device. In addition, the turn-on voltages (at which the luminance could be detected by the instrument) for coumarin 6 in BN<sub>1-3</sub> were 3.0, 4.0, and 4.0 V respectively, whereas for coumarin 6 in CBP, it was 4.5 V.

### 2.8. As a Light-Emitting Layer (EML) Material

The development of primary RGB emitters remains an important challenge to realize commercial full-color displays and lighting. In particular, it is difficult to generate high-performance blue emission because the intrinsically wide band gap makes it hard to inject charges into blue-emitting materials. As a result, the

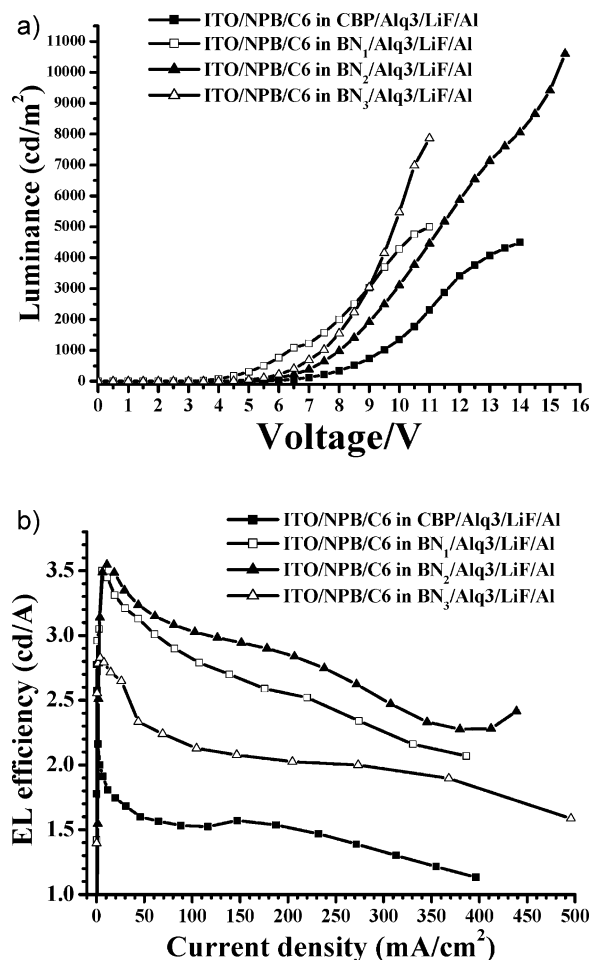


**Figure 9.** a) Luminance–voltage curves for the ITO/NPB (60 nm)/coumarin 6 (5%) doped in BN<sub>1-3</sub> or CBP (60 nm)/Alq<sub>3</sub> (60 nm)/LiF/Al (50 nm) devices, where BN<sub>1-3</sub> work as host materials. b) Efficiency–current density curves for the ITO/NPB (60 nm)/coumarin 6 (5%) doped in BN<sub>1-3</sub> or CBP (60 nm)/Alq<sub>3</sub> (60 nm)/LiF/Al (50 nm) devices.

performance of blue-light-emitting devices is usually not as good as that of their green or red counterparts. In addition, the National Television System Committee (NTSC) standard of color definition for displays imposes strict requirements for blue-emitting devices to obey. Because the power consumption of a full-color OLED is highly dependent upon the color of the blue emission, a pure/deep-blue color (the smaller the  $\gamma$ -value of the Commission Internationale de L'Eclairage (CIE), the deeper the blue emission) needs less power consumption in the device. Thus, developing deep-blue-color-emitting OLEDs is of particular importance in energy saving. However, in general, the main obstacles for realizing high-efficiency pure-blue OLEDs are the stringent requirements of the materials' high fluorescence quantum yield, wide-energy band gap, high thermal stability, and good thin-film morphology. Few materials have been able to meet these requirements so far. Thus, the preparation of novel pure/deep-blue-light-emitting materials exhibiting high efficiencies with a very-good CIE coordinate of  $\gamma < 0.15$  is greatly needed and is a main concern of the OLED field. Over the past few years, many

**Table 1.** PLQY (%) (at 313 nm excitation, in dichloromethane solution), HOMO level and decomposition point of the compounds.

Compound	PLQY [%]	HOMO [eV]	$T_d$ [°C]
NPB	16.08	5.47	410
BN <sub>1</sub>	80.57	5.67	485
BN <sub>2</sub>	83.49	5.97	492
BN <sub>3</sub>	52.86	5.71	545

blue emitters have been used, such as iridium(III)bis(4,6-difluorophenyl)-pyridinato-*N,C2'*picolinate (FIrpic),<sup>[9a,19]</sup> 4,4'-bis(2,2-diphenylethenyl)biphenyl (DPVBi),<sup>[20]</sup> spirofluorene,<sup>[21]</sup> big  $\pi$ -conjugating molecules like anthracene,<sup>[22]</sup> carbazole or triphenylamine modified molecules,<sup>[23]</sup> and aluminum, lithium and zinc complexes.<sup>[24]</sup> Of these materials, the blue-emitting, phosphorescent iridium complexes have attracted much attention. However, recently, some problems have been found in electrophosphorescence materials (PhOLEDs) for white lighting: the operational lifetimes are not as long as expected for this class of

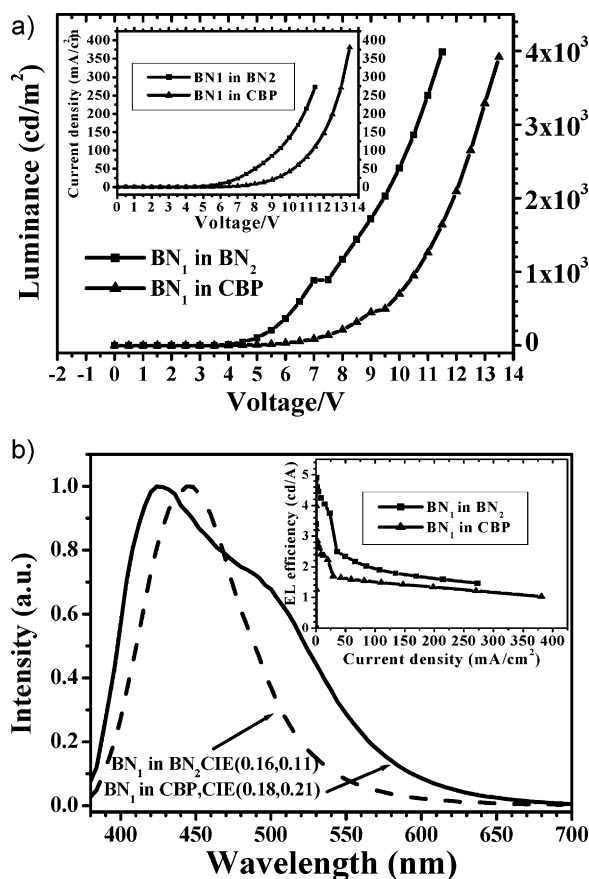


**Figure 10.** a) Luminance–voltage (and inset: current-density–voltage) curves for the ITO/NPB (30 nm)/BN<sub>1</sub> (30 nm)/BN<sub>1,3</sub> (5%) doped in BN<sub>2</sub> or CBP (60 nm)/Alq<sub>3</sub> (60 nm)/LiF/Al (50 nm) device, where BN<sub>1</sub> works first as the HTL then as the EML guest and BN<sub>2</sub> as the host for the EML. b) Electroluminescence spectra (and inset: efficiency–current density) curves for the ITO/NPB(30 nm)/BN<sub>1</sub>(30 nm)/BN<sub>1,3</sub> (5%) doped in BN<sub>2</sub> or CBP (60 nm)/Alq<sub>3</sub>(60 nm)/LiF/Al(50 nm) device.

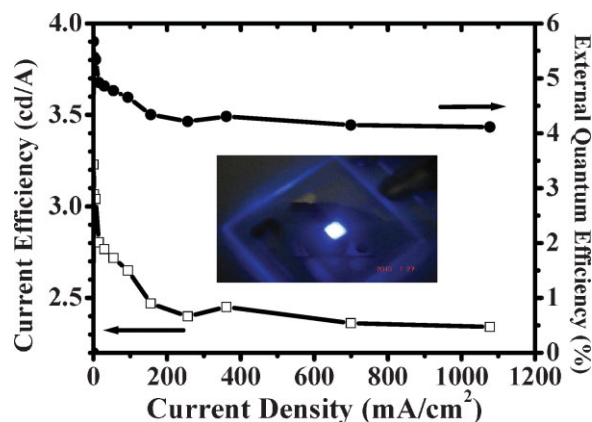


**Figure 11.** Current efficiency and external quantum efficiency plotted against current density for a device with the structure: ITO/NPB (50 nm)/BN<sub>1</sub> doped in BN<sub>2</sub> (20 nm)/TPBI (40 nm)/LiF (0.5 nm)/Al (150 nm). Inset: photo of a blue-emitting device.

materials, the cost of the noble iridium complexes is comparatively high and blue PhOLED emitters are relatively rare compared with the large number of green or red PhOLEDs. In addition, the external quantum efficiency of true blue PhOLEDs is not so high and they often exhibit a serious efficiency roll-off at high driving-current density due to triplet-triplet annihilation. Based on the above summary, the enthusiasm for PhOLEDs might diminish and that for electrofluorescent OLEDs (FLOLEDs) might revive instead.<sup>[21b,25]</sup>

Our experiments demonstrate that BNs have very-high PL efficiencies (Table 1). A rigid substitute, like carbazole, in BN<sub>2</sub> leads to a higher PL efficiency, while an electron-withdrawing group, like fluorine, in BN<sub>3</sub> reduces the PL efficiency. We therefore have used BNs as EMLs to fabricate OLEDs. Figure 10a demonstrates the luminance and current density vs. voltage and the inset of Figure 10b demonstrates the efficiency vs. current-density curves of a blue-emitting OLED with BN<sub>1</sub> doped in BN<sub>2</sub> or BN<sub>1</sub> doped in CBP as the EML. The highest luminance reached was 4000 cd cm<sup>-2</sup> at 11.5 V (273 mA cm<sup>-2</sup>) and the efficiency reached more than 4.9 cd A<sup>-1</sup> (8.6% external quantum efficiency) at 0.87 mA cm<sup>-2</sup>. After inserting a hole-blocking layer between the EML layer and the cathode (namely a TPBI layer between the BN<sub>1</sub> and the LiF (Fig. 11)), the highest luminance reached was 25 200 cd m<sup>-2</sup>. Although the highest efficiency, at 3.2 cd A<sup>-1</sup>, became smaller than for the device without the TPBI layer, the efficiency-versus-current-density curve remained stable until very-high current densities were reached (2.35 cd A<sup>-1</sup> at 1000 mA cm<sup>-2</sup> vs. 1.46 cd A<sup>-1</sup> at 272 mA m<sup>-2</sup> for ITO/NPB/BN<sub>1</sub> doped in BN<sub>2</sub>/Alq<sub>3</sub>/LiF/Al). This means that the efficiency does not roll off under high current densities. The emission of BN<sub>1</sub> doped in BN<sub>2</sub> was a pure, deep-blue color with CIE coordinates of (0.16, 0.11). (Fig. 10b)

### 3. Conclusions

We have synthesized a series of arylamine- or carbazole-modified binaphthyl derivatives that are versatile in OLED applications: they are efficient hole-transport, host and blue-light-emitting materials.

This three-in-one property may significantly reduce the cost of materials manufacture. In addition, they are a class of novel glassy materials: they do not have a unified melting point, can form thermally stable amorphous films and decompose at very-high temperatures. With BN<sub>1</sub> as the HTL, the current efficiency reached 8.03 cd A<sup>-1</sup>, 3 times higher than that of the device with NPB as the HTL (2.39 cd A<sup>-1</sup>). Moreover, by introducing NPB as a buffer layer and with BN<sub>1</sub> as the HTL, the maximum efficiency and luminance of the device, ITO/NPB/BN<sub>1</sub>/Alq<sub>3</sub>/LiF/Al, was further improved to 9.48 cd A<sup>-1</sup> and 25 300 cd m<sup>-2</sup> respectively. In addition, the lifetimes for BN<sub>1</sub>-based single-layer hole-only devices and multi-layer OLED devices with BN<sub>1</sub> as the HTL layer were longer than the counterpart NPB-based devices. As a host material, compared to the device with coumarin 6 as the emitting element in a CBP host, devices with coumarin 6 in a BN host exhibited a higher luminance and efficiency and a very-low onset voltage. As a light-emitting material, the PL quantum efficiencies for BN<sub>1-3</sub> in dichloromethane were very high due to the rigid binaphthyl backbone. The efficiency of the device with BN<sub>1</sub> doped in BN<sub>2</sub> as the EML reached 4.9 cd A<sup>-1</sup> (external efficiency 8.6%) at 0.87 mA cm<sup>-2</sup>, emitting a pure, deep-blue light (444 nm) with a CIE coordinate of (0.16, 0.11). By inserting a hole-blocking TPBI layer, the highest luminance reached more than 25 200 cd m<sup>-2</sup> and the highest efficiency reached 3.2 cd A<sup>-1</sup> (5.6% external efficiency). More importantly, the efficiency versus current density remained very stable through very-high current densities (2.35 cd A<sup>-1</sup> or 4.2% at 1000 mA cm<sup>-2</sup>).

## 4. Experimental

1,4-dibromobenzene, 1-bromo-4-fluorobenzene, diphenylamine, carbazole, *n*-BuLi, B(OCH<sub>3</sub>)<sub>3</sub>, 18-Crown-6, Pd(PPh<sub>3</sub>)<sub>4</sub> and NBS were bought from Alfa Aesar. 1,1'-binaphthyl-4,4'-diamine was purchased from Sinopharm Chemical Reagent Co. (SCRC). *N,N*-diphenyl-4-bromoaniline (**1**), 9-(*p*-bromophenyl)-9*H*-carbazole (**2**) and 9-(*p*-fluorophenyl)-9*H*-carbazole (**3**) were synthesized by the Ullmann reaction, a procedure that can be commonly found in the literature. For example, the procedure for the synthesis of compound **1** was as follows: 170 ml of *o*-xylene was added to a three-necked flask containing 35.3 g (125 mmol) of 1,4-dibromobenzene, 20.3 g (120 mmol) of diphenylamine, 2.1 g (12 mmol) of 1,10-phenanthroline, 6.5 g of CuBr and 10 g of KOH. The mixture was refluxed for 72 h under N<sub>2</sub> protection. After cooling, the organic phase was separated and condensed. Chromatography of the resulting residue on ~200–300 mesh silica gel with petroleum ether afforded a white powder. The solvent was evaporated and the solid was recrystallized in ethanol. White crystals were obtained.

Yield: 21.6 g, 63.5%; mp 124–125 °C; <sup>1</sup>H NMR (400 MHz, CDCl<sub>3</sub>, TMS, δ): 6.87 (d, *J* = 8.8, 2H), ~6.96–7.01 (m, 5H), ~7.16–7.20 (m, 5H), 7.25 (d, *J* = 7.6 Hz, 2H). ESI-MS (*m/z*): 323.65 [M]<sup>+</sup>; Anal. calcd for C<sub>18</sub>H<sub>14</sub>BrN: C 66.68, H 4.35, N 4.32; found: C 66.43, H 4.30, N 4.28.

For **2**, <sup>1</sup>H NMR (400 MHz, CDCl<sub>3</sub>, TMS, δ): 7.28 (d, *J* = 16.4 Hz, 2H), 7.45 (t, *J* = 11.6 Hz, 6H), 7.74 (d, *J* = 6.8 Hz, 2H); 8.14 (d, *J* = 6.8 Hz, 2H). ESI-MS (*m/z*): 345.97 [M + H + Na]<sup>+</sup>, 362.0 [M + H + K]<sup>+</sup>; Anal. calcd for C<sub>18</sub>H<sub>12</sub>BrN: C 67.10, H 3.75, N 4.35; found: C 65.65, H 3.23, N 4.22.

For **3**, <sup>1</sup>H NMR (400 MHz, CDCl<sub>3</sub>, TMS, δ): ~7.27–7.34 (m, 6H), 7.41 (t, *J* = 8.0 Hz, 2H), ~7.50–7.54 (m, 2H), 8.14 (d, *J* = 7.6 Hz, 2H). ESI-MS (*m/z*): 261.81 [M]<sup>+</sup>; Anal. calcd for C<sub>18</sub>H<sub>12</sub>FN: C 82.74, H 4.63, N 5.36; found: C 82.80, H 4.38, N 5.39.

**Synthesis of 3-Bromo-9-(*p*-fluorophenyl)-9*H*-carbazole (**4**):** 9.79 g (0.055 mol) of NBS were added slowly (over 1 h) to a three-necked flask, cooled by ice-salt and equipped with a magnetic stirrer, containing 13.05 g (0.05 mol) of **3**, 7 g of silica gel and 50 ml of CH<sub>2</sub>Cl<sub>2</sub>. After addition, the

stirring was continued for two and a half hours. 40 ml water was added to quench the reaction and the stirring was continued for another half hour with 20 ml of 1 N HCl addition. The solid substances were filtered off and then washed with CH<sub>2</sub>Cl<sub>2</sub> three times. The filtrate was transferred into a 500 ml separating funnel and extracted using 2 N HCl three times. The CH<sub>2</sub>Cl<sub>2</sub> was rotated and a pale-yellow oil was obtained. The oil was recrystallized in hexane and a white solid product was obtained.

Yield: 9.54 g, 56%; mp 79–80 °C; <sup>1</sup>H NMR (400 MHz, CDCl<sub>3</sub>, TMS, δ): 7.19 (d, *J* = 8.8, 1 H), ~7.28–7.33 (m, 4 H), 7.43 (d, *J* = 7.6 Hz, 1 H), ~7.46–7.51 (m, 3 H), 8.09 (d, *J* = 7.6 Hz, 2 H), 8.25 (s, 1 H); ESI-MS (*m/z*): 362.01 [M + Na]<sup>+</sup>; Anal. calcd for C<sub>18</sub>H<sub>11</sub>BrFN: C 63.55, H 3.26, N 4.12; found: C 63.15, H 2.77, N 4.12.

**General Procedure for the Synthesis of 5, 6, and 7:** *n*-BuLi was added slowly into a three-necked flask, protected by N<sub>2</sub> and cooled by dry-ice (–78 °C), containing 10 mmol of Ar-Br (**1**, **2** or **4**) and 50 ml of tetrahydrofuran (THF). The reaction was kept at –78 °C for 1 h. 30 mmol of B(OCH<sub>3</sub>)<sub>3</sub> were added rapidly to the flask and the reaction continued for 2 h. As the temperature was raised to 0 °C, 50 ml of 2 N HCl was added to the flask and the reaction continued for another 3 h. Ether was used to extract the product and was rotated to dryness. White powders were obtained.

**4,4'-Di-iodobinaphthyl (**8**):** 11.38 g (40 mol) of 1,1'-binaphthyl-4,4'-diamine were added to a 250 ml three-necked flask containing 30 ml of HCl and 30 ml of water, and the solution was stirred. The flask was cooled to less than 5 °C by ice-salt, and stirred for 1 h. 5.87 g (85 mmol) of NaNO<sub>2</sub> solved in 10 ml of water were added slowly to the flask to proceed the diazotiation until the KI-starch turned blue. The temperature was managed to be kept below –5 °C and stirring continued for another 30 min. A brilliant-yellow diazotiated solution was obtained and was kept in the refrigerator. Then, the diazotiated solution was added slowly to a three-necked flask containing 13.28 g (80 mmol) of KI and 10 ml of water. A yellowish-brown solid appeared and nitrogen was released. After addition, the stirring was continued for 4 h, and the temperature was slowly raised to 50–60 °C until no further nitrogen was released. 20% NaOH solution was added to make the solution slightly basic. The solution was filtered and the yellowish-brown solid was washed with water. The dried solid was train-sublimated and small, yellow crystals were obtained.

Yield: 12.33 g, 61%; mp 229–230 °C; <sup>1</sup>H NMR (400 MHz, CDCl<sub>3</sub>, TMS, δ): 7.17 (d, *J* = 7.2 Hz, 2H), ~7.26–7.34 (m, 4H), ~7.55–7.59 (m, 2H), 8.20 (d, *J* = 7.6 Hz, 4H); ESI-MS (*m/z*): 507.11 [M + H]<sup>+</sup>, 382.01 [M – I + H]<sup>+</sup>; Anal. calcd for C<sub>20</sub>H<sub>12</sub>I<sub>2</sub>: C 47.46, H 2.39; found: C 47.62, H 2.52.

**4',4''-N,N-diphenylamine-4,4'-diphenyl-1,1'-binaphthyl (BN1), 4',4''-(9*H*-9-carbazole)-4,4'-diphenyl-1,1'-binaphthyl (BN2), 4,4' bis(9-(*p*-fluorophenyl)-9*H*-3-carbazole)-1,1'-binaphthyl (BN3):** 0.25 g (0.2 mmol) of Pd(PPh<sub>3</sub>)<sub>4</sub> and 1.3 g (12.0 mmol) of Na<sub>2</sub>CO<sub>3</sub> saturated solution were added to a three-necked flask containing 1.01 g (2.0 mmol) of **8**, 1.35 g (5.0 mmol) of Ar-B(OH)<sub>2</sub> (**5**, **6**, **7**), 60 ml of toluene and 20 ml of ethanol. The mixture was refluxed for 19 h. After that, the organic phase was separated and condensed. Chromatography of the resulting residue on a ~200–400 mesh silica gel with toluene afforded BN<sub>1-3</sub>. The solvent was evaporated and the solid was recrystallized in ethanol. A white powder was obtained.

For BN<sub>1</sub>, yield: 75.6%; <sup>1</sup>H NMR (400 MHz, CDCl<sub>3</sub>, TMS, δ): 7.34 (t, *J* = 7.2 Hz, 4 H), 7.41 (t, *J* = 4.8 Hz, 2 H), 7.49 (t, *J* = 8.0 Hz, 4 H), 7.55 (t, *J* = 7.6 Hz, 2 H), 7.63 (t, *J* = 8.4 Hz, 6 H), ~7.66–7.71 (m, 4 H), 7.77 (d, *J* = 7.6 Hz, 4 H), 7.87 (d, *J* = 7.6 Hz, 4 H), 8.19 (t, *J* = 7.2 Hz, 6 H); ESI-MS (*m/z*): 764.73 [M + H + Na]<sup>+</sup>; Anal. calcd for C<sub>56</sub>H<sub>40</sub>N<sub>2</sub>: C 90.78, H 5.44, N 3.78; found: C 90.17, H 5.69, N 3.70.

For BN<sub>2</sub>, yield: 82.3%; <sup>1</sup>H NMR (400 MHz, CDCl<sub>3</sub>, TMS, δ): 7.34 (t, *J* = 7.2 Hz, 4 H), 7.41 (t, *J* = 4.8 Hz, 2 H), 7.49 (t, *J* = 8.0 Hz, 4 H), 7.55 (t, *J* = 7.6 Hz, 2 H), 7.63 (t, *J* = 8.4 Hz, 6 H), ~7.66–7.71 (m, 4 H), 7.77 (d, *J* = 7.6 Hz, 4 H), 7.87 (d, *J* = 7.6 Hz, 4 H), 8.19 (t, *J* = 7.2 Hz, 6 H); ESI-MS (*m/z*): 774.79 [M + K]<sup>+</sup>; Anal. calcd for C<sub>56</sub>H<sub>36</sub>N<sub>2</sub>: C 91.27, H 4.92, N 3.80; found: C 90.64, H 4.98, N 3.74.

For BN<sub>3</sub>, yield: 82.3%; <sup>1</sup>H NMR (400 MHz, CDCl<sub>3</sub>, TMS, δ): 8.41 (s, 2 H), 8.18 (q, *J* = 12.2 Hz, 4 H), 7.66 (m, 14 H), 7.48 (m, 8 H), 7.34 (m, 4 H); ESI-MS (*m/z*): 774.66 [M + H]<sup>+</sup>; Anal. calcd for C<sub>56</sub>H<sub>34</sub>N<sub>2</sub>F<sub>2</sub>: C 87.03, H 4.43, N 3.62; found: C 86.32, H 3.46, N 4.94.

## Acknowledgements

This work was financially supported by NSFC 60868001, the National High-Technology Research and Development Program of China (2008AA03A331), the Key Project of the Shanghai Education Committee (08ZZ42), and the Science and Technology Commission of the Shanghai Municipality (08PJ14053, 08DZ1140702). Supporting Information is available online from Wiley InterScience or from the author.

Received: February 12, 2010  
Published online: June 24, 2010

- [1] a) Y. R. Sun, N. C. Giebink, H. Kanno, B. W. Ma, M. E. Thompson, S. R. Forrest, *Nature (London)* **2006**, *440*, 908; b) M. A. Baldo, D. F. O'Brien, Y. You, A. Shoustikov, S. Sibley, M. E. Thompson, S. R. Forrest, *Nature (London)* **1998**, *395*, 151; c) X. C. Gao, H. Cao, C. H. Huang, B. G. Li, S. Umitani, *Appl. Phys. Lett.* **1998**, *72*, 2217; d) C. W. Tang, S. A. VanSlyke, *Appl. Phys. Lett.* **1987**, *51*, 913.
- [2] Y. Hamada, T. Sano, K. Shibata, K. Kuroki, *Jpn. J. Appl. Phys.* **1995**, *34*, L824.
- [3] a) P. N. M. dos Anjos, H. Aziz, N. Hu, Z. D. Popovic, *Org. Electron.* **2003**, *3*, 9; b) S. A. Van Slyke, C. H. Chen, C. W. Tang, *Appl. Phys. Lett.* **1996**, *69*, 2160.
- [4] Z. D. Popovic, in: *Proc. SPIE, Vol. 3476: Organic Light-Emitting Materials and Devices II* (Ed: Z. H. Kafafi), San Diego, CA July **1998**, p. 68.
- [5] Z. Wang, S. Naka, H. Okada, *Thin Solid Films* **2009**, *518*, 497.
- [6] a) S. C. Xia, R. C. Kwong, V. I. Adamovich, M. S. Weaver, J. J. Brown, in *Reliability Physics Symp., 2007, Proc. 45th Annual IEEE Int.* **2007**, p. 253; b) Y. Liew, H. Aziz, N. Hu, H. Chan, G. Xu, Z. Popovic, *Appl. Phys. Lett.* **2000**, *77*, 2650.
- [7] P. Cusumano, F. Buttitia, A. Di Cristofalo, C. Calì, *Synth. Met.* **2003**, *139*, 657.
- [8] a) A. Pinato, A. Cester, M. Meneghini, N. Wrachien, A. Tazzoli, S. Xia, V. Adamovich, M. S. Weaver, J. J. Brown, E. Zanoni, G. Meneghesso, *IEEE Trans. Electron Devices* **2010**, *57*, 178; b) F. P. Rosselli, W. G. Quirino, C. Legnani, V. L. Calil, K. C. Teixeira, A. A. Leit, R. B. Capaz, M. Cremona, C. A. Achete, *Org. Electron.* **2009**, *10*, 1417; c) S. Scholz, B. Lussem, K. Leo, *Appl. Phys. Lett.* **2009**, *95*, 183309; d) V. V. Jarikov, D. Y. Kondakov, *J. Appl. Phys.* **2009**, *105*, 034905; e) L. J. Soltzberg, J. D. Slinker, S. F. Torres, D. A. Bernards, G. G. Malliaras, H. D. Abrun, J. S. Kim, R. H. Friend, M. D. Kaplan, V. Goldberg, *J. Am. Chem. Soc.* **2006**, *128*, 7761; f) Z. D. Popovic, H. Aziz, *IEEE J. Selected Topics Quantum Electron.* **2002**, *8*, 362; g) H. Aziz, Z. D. Popovic, N. X. Hu, A. M. Hor, G. Xu, *Science* **1999**, *283*, 1900.
- [9] a) V. Sivasubramaniam, F. Brodtkorb, S. Hanning, O. Buttler, H. P. Loeb, V. Elsbergen, H. Boerner, U. Scherf, M. Kreyenschmidt, *Solid State Sci.* **2009**, *11*, 1933; b) D. Y. Kondakov, R. H. Young, *SID Int. Symp. Dig. Technical Papers* **2009**, *XL*, 687; c) D. Y. Kondakov, *J. Appl. Phys.* **2008**, *104*, 084520; d) T. Matsushima, H. Murata, *J. Appl. Phys.* **2008**, *104*, 034507; e) Y. J. Lee, H. Lee, Y. Byun, S. Song, J. E. Kim, D. Eom, W. Cha, S. S. Park, J. Kim, H. Kim, *Thin Solid Films* **2007**, *515*, 5674; f) R. P. Tang, Z. A. Tan, Y. F. Li, F. Xi, *Chem. Mater.* **2006**, *18*, 1053; g) J. Y. Li, D. Liu, Y. Q. Li, C. S. Lee, H. L. Kwong, S. T. Lee, *Chem. Mater.* **2005**, *17*, 1208; h) P. Kundu, K. R. J. Thomas, J. T. Lin, Y. T. Tao, C. H. Chien, *Adv. Funct. Mater.* **2003**, *13*, 445; i) D. Y. Kondakov, J. R. Sandifer, C. V. Tang, H. J. Young, *J. Appl. Phys.* **2003**, *93*, 1108; j) L.-H. Chan, R.-H. Lee, C.-F. Hsieh, H.-C. Yeh, C.-T. Chen, *J. Am. Chem. Soc.* **2002**, *124*, 6469; k) D. E. Loy, B. E. Koene, M. E. Thompson, *Adv. Funct. Mater.* **2002**, *12*, 245; l) Z. D. Popovic, H. Aziz, N. Hu, A. Ioannidis, P. N. M. dos Anjos, *J. Appl. Phys.* **2001**, *89*, 4673; m) F. Steuber, J. Staudigel, M. Stossel, J. Simmerer, A. Winnacker, H. Spreitzer, F. Weissortel, J. Salbeck, *Adv. Mater.* **2000**, *12*, 130; n) B. E. Koene, D. E. Loy, M. E. Thompson, *Chem. Mater.* **1998**, *10*, 2235; o) D. F. O'Brien, P. Burrows, S. R. Forrest, B. E. Koene, D. E. Loy, M. E. Thompson, *Adv. Mater.* **1998**, *10*, 1108; p) H. Vestweber, W. Rieß, *Synth. Met.* **1997**, *91*, 81; q) H. Tanaka, S. Tokito, Y. Taga, A. Okada, *Chem. Commun.* **1996**, 2175; r) S. Tokito, H. Tanaka, A. Okada, Y. Taga, *Appl. Phys. Lett.* **1996**, *69*, 878; s) C. Adachi, K. Nagai, N. Tamoto, *Appl. Phys. Lett.* **1995**, *66*, 2679; t) A. Higuchi, H. Inada, T. Kobata, Y. Shirota, *Adv. Mater.* **1991**, *3*, 549.
- [10] S. A. Vanslyke, C. H. Chen, C. W. Tang, *Appl. Phys. Lett.* **1996**, *65*, 2160.
- [11] a) L. Q. Huang, Y. Z. Liu, C. J. Yang, C. Yi, J. Liu, P. Qiu, X. C. Gao, *Huaxue Shiji (Chem. Reagents)*, **2006**, *28*, 290; b) L. Q. Huang, Y. Z. Liu, C. J. Yang, C. Yi, J. Liu, X. C. Gao, *Gongneng Cailiao yu Qijian Xuebao (J. Funct. Mater. Devices)*, **2006**, *12*, 451; c) X. C. Gao, L. Q. Huang, CN 1775738, **2006**.
- [12] Q. G. He, H. Z. Lin, Y. F. Weng, B. Zhang, Z. M. Wang, G. T. Lei, L. D. Wang, Y. Qiu, F. L. Bai, *Adv. Funct. Mater.* **2006**, *16*, 1343.
- [13] X. C. Gao, CN 200520098133.3, **2006**.
- [14] R. Dawson, M. W. Windsor, *J. Phys. Chem.* **1968**, *72*, 3251.
- [15] a) Y. Liu, K. Ye, Y. Fan, W. F. Song, W. Wang, Z. Hou, *Chem. Commun.* **2009**, 3699; b) B. Lim, J. T. Hwang, J. Y. Kim, J. Ghim, D. Vak, Y. Y. Noh, S. Hyoung Lee, K. Lee, A. J. Heeger, D. Y. Kim, *Org. Lett.* **2006**, *8*, 4703; c) Z. H. Li, M. S. Wong, H. Fukutani, Y. Tao, *Org. Lett.* **2006**, *8*, 4271; d) S. Ito, T. Kubo, N. Morita, T. Ikoma, S. Tero-Kubota, J. Kawakami, A. Tajiri, *J. Org. Chem.* **2005**, *70*, 2285; e) J. Wu, M. Baumgarten, M. G. Debije, J. M. Warman, K. Müllen, *Angew. Chem.* **2004**, *116*, 5445; f) R. D. Hrehca, C. P. George, A. Haldi, B. Domercq, M. Malagoli, S. Barlow, J. L. Brédas, B. Kippelen, S. R. Marder, *Adv. Funct. Mater.* **2003**, *13*, 967; g) H. Zhao, C. Tanjutco, S. Thayumanavan, *Tetrahedron Lett.* **2001**, *42*, 4421; h) J. Louie, J. F. Hartwig, *J. Am. Chem. Soc.* **1997**, *119*, 11695; i) Y. Shirota, Y. Kuwabara, H. Inada, T. Wakimoto, H. Nakada, Y. Yonemoto, S. Kawami, K. Imai, *Appl. Phys. Lett.* **1997**, *65*, 807; j) Y. Shirota, Y. Kuwabara, D. Okuda, R. Okuda, H. Ogawa, H. Inada, T. Wakimoto, H. Nakada, Y. Yonemoto, S. Kawami, K. Imai, *J. Lumin.* **1997**, *72*, 985; k) H. Kageyama, K. Itano, W. Ishikawa, Y. Shirota, *J. Mater. Chem.* **1996**, *6*, 675; l) C. Adachi, K. Nagai, N. Tamoto, *Appl. Phys. Lett.* **1995**, *66*, 2679; m) W. Ishikawa, K. Noguchi, Y. Kuwabara, Y. Shirota, *Adv. Mater.* **1993**, *5*, 559; n) A. Higuchi, H. Inada, T. Kobata, Y. Shirota, *Adv. Mater.* **1991**, *3*, 549.
- [16] F. Papadimitrakopoulos, X.-M. Zhang, D. L. Thomsen, III, K. A. Higginson, *Chem. Mater.* **1996**, *8*, 1363.
- [17] a) B. Wei, K. Furukawa, J. Amagai, M. Ichikawa, T. Koyama, Y. Taniguchi, *Semicond. Sci. Technol.* **2004**, *19*, L56; b) G. G. Malliaras, Y. Shen, D. H. Dunlap, H. Murata, Z. H. Kafafi, *Appl. Phys. Lett.* **2001**, *79*, 2582; c) P. M. Borsenberger, E. H. Magin, M. Der VanAuerwaer, F. C. De Schryver, *Phys. Status Solidi A* **1993**, *140*, 9; d) W. Blom, M. J. M. de Jong, M. G. van Munster, *Phys. Rev. B: Condens. Matter* **1997**, *55*, R656.
- [18] a) Y. W. Park, Y. M. Kim, J. H. Choi, B. K. Ju, *J. Nanosci. Nanotechnol.* **2009**, *9*, 1607; b) Y. Tao, Q. Wang, Y. Shang, C. Yang, L. Ao, J. Qin, D. G. Ma, Z. G. Shuai, *Chem. Commun.* **2009**, 77; c) V. Jankus, C. Winscom, A. P. Monkman, *J. Chem. Phys.* **2009**, *130*, 074501; d) W. S. Han, H. J. Son, K. R. Wee, K. T. Min, S. Kwon, I. H. Suh, S. H. Choi, D. H. Jung, S. O. Kang, *J. Phys. Chem. C* **2009**, *113*, 19686; e) S. Y. Takizawa, V. A. Montes, P. Anzenbacher, *J. Chem. Mater.* **2009**, *21*, 2452; f) H. S. Bang, D. C. Choo, T. W. Kim, J. H. Park, J. H. Seo, Y. K. Kim, *Mol. Cryst. Liq. Cryst.* **2009**, *498*, 265; g) M. E. Kondakova, T. D. Pawlik, R. H. Young, D. J. Giesen, D. Y. Kondakov, C. T. Brown, J. C. Deaton, J. R. Lenhard, K. P. Klubik, *J. Appl. Phys.* **2008**, *104*, 094501; h) H. Tang, X. R. Wang, Y. Li, W. G. Wang, R. G. Sun, *Displays* **2008**, *29*, 502.
- [19] a) J. H. Lee, J. I. Lee, J. Y. Lee, H. Y. Chu, *Org. Electron.* **2009**, *10*, 1529; b) X. N. Li, Z. J. Wu, Z. J. Si, H. J. Zhang, L. Zhou, X. J. Liu, *Inorg. Chem.* **2009**, *48*, 7740; c) M. H. Tsai, T. H. Ke, H. W. Lin, C. C. Wu, S. F. Chiu, F. C. Fang, Y. L. Liao, K. T. Wong, Y. H. Chen, C. I. Wu, *Appl. Mater. Interfaces* **2009**, *1*, 567; d) K. R. Wee, W. S. Han, H. J. Son, S. N. Kwon, S. O. Kang, *J. Phys. D: Appl. Phys.* **2009**, *42*, 235107; e) M. T. Chu, M. T. Lee, C. H. Chen, M. R. Tseng, *Org. Electron.* **2009**, *10*, 1158; f) J. J. Lin, W. S. Liao, H. J. Huang, F. Wu, C. H. Cheng, *Adv. Funct. Mater.* **2008**, *18*, 485; g) H. Fukagawa, K. Watanabe, T. Szuzuki, S. Tokito, *Appl. Phys. Lett.* **2008**, *93*, 133312; h) S. H. Eom, Y. Zheng, N. Chopra, J. Lee, F. So, J. Xue, *Appl. Phys. Lett.* **2008**, *93*, 133309; i) S. J. Su, E. Gonmori, H. Sasabe, J. Kido, *Adv. Mater.* **2008**, *20*, 4189; j) P. I. Shih, C. H. Chien, C. Y. Chuang, C. F. Shu,

- C. H. Yang, J. H. Chen, Y. Chi, *J. Mater. Chem.* **2007**, *17*, 1692; k) S. J. Yeh, M. F. Wu, C. T. Chen, Y. H. Song, Y. Chi, M. H. Ho, S. F. Hsu, C. H. Chen, *Adv. Mater.* **2005**, *17*, 285; l) X. Ren, J. Li, R. J. Holmes, P. I. Djurovich, S. R. Forrest, M. E. Thompson, *Chem. Mater.* **2004**, *16*, 4743; m) R. J. Holmes, S. R. Forrest, Y. J. Tung, R. C. Kwong, J. J. Brown, S. Garon, M. E. Thompson, *Appl. Phys. Lett.* **2003**, *82*, 2422; n) S. Tokito, T. Iijima, Y. Suzuri, H. Kita, T. Tsuzuki, F. Sato, *Appl. Phys. Lett.* **2003**, *83*, 569; o) R. J. Holmes, B. W. D'Andrade, X. Ren, J. Li, M. E. Thompson, S. R. Forrest, *Appl. Phys. Lett.* **2003**, *83*, 3818.
- [20] a) C. J. Huang, C. C. Kang, T. C. Lee, W. R. Chen, T. H. Meen, *J. Lumin.* **2009**, *129*, 1292; b) C. J. Huang, T. H. Meen, K. C. Liao, Y. K. Su, *J. Phys. Chem. Solids* **2009**, *70*, 765; c) G. Cheng, Z. Q. Xie, Y. F. Zhang, H. Xia, Y. G. Ma, S. Y. Liu, *Semicond. Sci. Technol.* **2005**, *20*, L23; d) G. Cheng, F. He, Y. Zhao, Y. Duan, H. Q. Zhang, B. Yang, Y. G. Ma, S. Y. Liu, *Semicond. Sci. Technol.* **2004**, *19*, L78; e) H. Tokailin, H. Higashi, C. Hosokawa, T. Kusumoto, *Proc. SPIE, Vol. 1910: Electroluminescent Mater., Devices, Large-Screen Displays* **1993**, 38.
- [21] a) G. S. Chaurasia, M. Dixit, V. Kumar, S. Prakash, B. Jena, J. K. Verma, M. Jain, R. S. Anand, S. S. Manoharan, *Org. Lett.* **2009**, *11*, 1290; b) C. C. Chi, C. L. Chiang, S. W. Liu, H. Yueh, C. T. Chen, C. T. Chen, *J. Mater. Chem.* **2009**, *19*, 5561; c) R. Pudzich, J. Salbeck, *Synth. Met.* **2003**, *138*, 21; d) C. C. Wu, Y. T. Lin, H. H. Chiang, T. Y. Cho, C. W. Chen, K. T. Wong, Y. L. Liao, G. H. Lee, S. M. Peng, *Appl. Phys. Lett.* **2002**, *81*, 577; e) J. Salbeck, N. Yu, J. Bauer, F. W. Grtel, H. Bestgen, *Synth. Met.* **1997**, *91*, 209.
- [22] a) C. H. Chien, C. K. Chen, F. M. Hsu, C. F. Shu, P. T. Chou, C. H. Lai, *Adv. Funct. Mater.* **2009**, *19*, 560; b) S. Liu, P. Jiang, G. Song, R. Liu, H. J. Zhu, *Dyes Pigments* **2009**, *81*, 218; c) Y. M. Jeon, J. W. Kim, C. W. Lee, M. S. Gong, *Dyes Pigments* **2009**, *83*, 66; d) J. Y. Yu, M. J. Huang, C. H. Chen, C. S. Lin, C. H. Cheng, *J. Phys. Chem. C* **2009**, *113*, 7407; e) M. T. Li, W. L. Li, W. M. Su, F. X. Zang, B. Chu, Q. Xin, D. F. Bi, B. Li, T. Z. Yu, *Solid State Electron.* **2008**, *52*, 121; f) S. K. Kim, B. Yang, Y. G. Ma, J. H. Lee, J. W. Park, *J. Mater. Chem.* **2008**, *18*, 3376; g) X. H. Zhang, M. W. Liu, O. Y. Wong, C. S. Lee, H. L. Kwong, S. T. Lee, S. K. Wu, *Chem. Phys. Lett.* **2003**, *369*, 478; h) X. Y. Jiang, Z. L. Zhang, X. Y. Zheng, Y. Z. Wu, S. H. Xu, *Thin Solid Films* **2001**, *401*, 251.
- [23] a) R. M. Adhikari, L. Duan, L. D. Hou, Y. Qiu, D. C. Neckers, B. K. Shah, *Chem. Mater.* **2009**, *21*, 4638; b) R. M. Adhikari, D. C. Neckers, *J. Org. Chem.* **2009**, *74*, 3341; c) Y. T. Tao, Q. Wang, Y. Shang, C. Y. L. Ao, J. Qin, D. G. Ma, Z. G. Shuai, *Chem. Commun.* **2009**, 77; d) S. K. Kim, B. Yang, Y. I. Park, Y. G. Ma, J. Y. Lee, H. J. Kim, J. Park, *Org. Electron.* **2009**, *10*, 822; e) Y. T. Tao, Q. Wang, Y. Shang, C. L. Yang, L. Ao, J. G. Qin, D. G. Ma, Z. G. Shuai, *Chem. Commun.* **2009**, 77; f) S. L. Tao, Y. C. Zhou, C. S. Lee, S. T. Lee, D. Huang, X. H. Zhang, *J. Phys. Chem. C* **2008**, *112*, 14603; g) Z. Q. Gao, Z. H. Li, P. F. Xia, M. S. Wong, K. W. Cheah, C. H. Chen, *Adv. Funct. Mater.* **2007**, *17*, 3194; h) K. Kreger, M. Bate, C. Neuber, H. W. Schmidt, P. Strohhriegel, *Adv. Funct. Mater.* **2007**, *17*, 3456; i) Q. Fang, B. Xu, B. Jiang, H. T. Fu, W. Q. Zhu, X. Y. Jiang, Z. L. Zhang, *Synth. Met.* **2005**, *155*, 206; 23 L. H. Chan, R. H. Lee, C. F. Hsieh, H. C. Yeh, C. T. Chen, *J. Am. Chem. Soc.* **2002**, *124*, 6469.
- [24] a) S. H. Liao, J. R. Shiu, S. W. Liu, S. J. Yeh, Y. H. Chen, C. T. Chen, T. J. Chow, C. I. Wu, *J. Am. Chem. Soc.* **2009**, *131*, 763; b) H. Wang, B. S. Xu, X. G. Liu, H. F. Zhou, Y. Y. Hao, H. X. Xu, L. Q. Chen, *Org. Electron.* **2009**, *10*, 918; c) G. Wang, Y. He, *Mater. Lett.* **2009**, *63*, 470; d) J. C. Deaton, D. W. Place, C. T. Brown, M. Rajeswaran, M. E. Kondakova, *Inorg. Chim. Acta* **2008**, *361*, 1020.
- [25] a) V. Sivasubramaniam, F. Brodtkorb, S. Hanning, H. P. Loebl, V. V. Elsbergen, H. Boerner, U. Scherf, M. Kreyenschmidt, *J. Fluorine Chem.* **2009**, *130*, 640; b) C.-F. Chang, Y.-M. Cheng, Y. Chi, Y.-C. Chiu, C.-C. Lin, G.-H. Lee, P.-T. Chou, C.-C. Chen, C.-H. Chang, C.-C. Wu, *Angew. Chem. Int. Ed.* **2008**, *47*, 4542; c) C.-H. Yang, Y.-M. Cheng, Y. Chi, C.-J. Hsu, F.-C. Fang, K.-T. Wong, P.-T. Chou, C.-H. Chang, M.-H. Tsai, C.-C. Wu, *Angew. Chem. Int. Ed.* **2007**, *46*, 2418; d) S.-J. Yeh, C.-T. Chen, Y.-H. Song, Y. Chi, M.-H. Ho, *J. Soc. Information Display* **2005**, *13*, 857; e) R. J. Holmes, S. R. Forrest, T. Sajoto, A. Tamayo, P. I. Djurovich, M. E. Thompson, J. Books, Y.-J. Tung, B. W. D'Andrade, M. S. Weaver, R. C. Kwong, J. J. Brown, *Appl. Phys. Lett.* **2005**, *87*, 243507.